ISSN 0003-6838, Applied Biochemistry and Microbiology, 2024, Vol. 60, No. 2, pp. 287–293. © Pleiades Publishing, Inc., 2024.

Structural and Functional Impacts of Extended N-Terminal End of the Small Heat Shock Protein *Tpv* HSP 14.3

S. Zabci[a], * and S. Kocabiyik[a]

[a] *Department of Biological Sciences, Faculty of Arts and Science, Middle East Technical University, Ankara, Turkey*

**e-mail: sema.zabc@yahoo.com*

Received July 25, 2023; revised September 12, 2023; accepted November 5, 2023

Abstract—Small heat shock proteins (sHSPs) are composed of the α-crystallin domain, which is highly conserved, and variable N-terminal and C-terminal domains. In contrast to the α-crystallin domain, structures of the flanking N- and C-terminal domains are poorly defined. The N-terminal domain is the most divergent region in sequence and length among small heat shock proteins. In this study, to provide further insight into the importance of N-terminal tags in the chaperone function of small heat shock proteins, two variants of *Tpv* HSP 14.3 containing polyhistidine tags (11-aa and 26-aa in length) in the proximal part of their N-termini were used. These variants were generated by expressing the cloned *Tpv* HSP 14.3 gene in *Escherichia coli* using the expression vectors pQE-31 and TAGZyme pQE-2. The His-tagged recombinant proteins were purified by affinity chromatography. The effects of poly-His tags on chaperone activity of the *Tpv* HSP 14.3 were evaluated using pig heart citrate synthase as the model substrate. The results showed that *Tpv* HSP 14.3 variants with N-terminal tags were more effective chaperones than the one without tag. In addition, the alterations in intrinsically disordered states of N-termini were analyzed by means of the PONDR predictor. The results indicated that the disordered nature of the fused tags and additional hydrophobic residues they contributed to the N terminus may increase the capacity of *Tpv* HSP 14.3 to interact with its substrate protein and thereby improve its chaperone activity.

Keywords: small heat shock protein (sHSP), N-terminal domain, *Thermoplasma volcanium*, His-tag, intrinsically disordered region, 3-D modelling

DOI: 10.1134/S0003683824020200

Small heat shock proteins (sHSPs), together with the closely related vertebrate α-crystallins, are constituting a unique family of molecular chaperones that prevent the accumulation of damaged proteins in an ATP-independent manner. The subsequent refolding can be achieved by major chaperone families like HSP70/HSP27 [1]. The formation of dimers, which is a typical feature of all sHSPs, is the first step in hierarchical assembly of the higher-order oligomers (from 9 to 40 subunits). sHSPs are organized in three partite domains: a central structurally well-conserved α-crystalline domain (ACD) and flanking variable N-terminal domain (NTD), and a C-terminal domain (CTD) [2]. In contrast to the well-defined ACD, structural information regarding N- and C-termini is relatively limited. The NTD is the most diverse region in sequence and length among all sHSPs [2–6]. The high flexibility of this region, as well as its susceptibility to proteolysis, are the main limitations to obtain high-quality crystallographic data. The exceptions are N-termini of TaHSP 16.9 from wheat, TSP36 from the beef tapeworm *Taenia saginata*, and HSP 14.0 from *Sulfolobolus tokodaii*. As revealed by their well-resolved crystal structures, they appear to be intrinsically disordered with a tendency to form α-helices [7–9]. The NTD exchange, truncation, cross-linking, and amino acid substitution studies indicated that this region may potentially be important for substrate recognition and binding [3, 10–13]. In addition, there are reports indicating that stress signals, such as high temperature or NTD phosphorylation, destabilize the oligomeric structure of sHSP [14, 15]. Disintegration of oligomers leads to exposure of hydrophobic interior surface, including NTD, and enhances substrate protein binding [16]. Overall, these results suggest that NTD is involved in oligomer organization and stability. Consistent with this notion, extension of the N-terminus in HSP 16.5 (from *Methanocaldococcus jannaschii*) resulted in the formation of polydisperse oligomers with greater substrate binding affinity [17]. This modification was achieved by inserting the Pro-rich 14-amino acid long peptide, which is specific for the human Hsp27 located near the junction of NTD and ACD of HSP 16.5.

To address the lack of reports on the effect of N-terminal tags in contributing to the chaperone activity of sHSPs, in this study, we used two NTD variants of the *Tpv* HSP 14.3 (from the thermoacidophilic archaeon

Thermoplasma volcanium) containing His-rich tags in the proximal part of its N-terminus. These variants were generated by use of commercially available vectors, which are commonly used in various expression systems. The poly-His tags differed in length, number of His residues, amino acid composition, and charge density. Chaperone activities of the variants with the poly-His tags as compared to the variant without tag, were investigated for protection of the model substrate pig heart citrate synthase (phCS) against heat inactivation. In addition, the magnitude of change in the structure of NTD with respect to the intrinsically disordered state was analyzed by means of the PONDR predictor.

MATERIALS AND METHODS

Plasmid constructs. Two of the N-terminal variants were generated by modifications at the DNA level as follows: the TVN0775 gene (locus name TVG_RS04180, sequences 790978...791352) of *T. volcanium* encoding the recombinant sHSP, *Tpv* HSP 14.3, was previously sub-cloned into pQE-31 expression vector (pQE-31/*Tpv* HSP14.3) for expression in *Escherichia coli* [18]. The expressed 6xHis-tagged fusion protein contained the 26-aa N-terminal extension (*Tpv* HSP 14.3 variant 1), which was one of the N-terminal variants used in the present study. The second variant was constructed using the TAGZyme pQE-2 expression vector system (QIAGEN Inc., USA). The *Tpv* HSP 14.3 gene was amplified from the *T. volcanium* genomic DNA by PCR (Gene cycler, Techne Inc., USA) using the forward primer 5'-T GAG CAT ATG CAG ATG TAT ACA CCC ATA AAG TTC TTT ACG-3' including *Nde*I recognition site and the reverse primer 5'-TGAG CTG CAG C ACC CAA TCA CAT CAA GCA TAC-3' including *Pst*I recognition site. Restriction enzyme sites are underlined in the above mentioned forward and reverse primer sequences. The PCR amplicon after purification (QIAquick Gel Extraction Kit, QIAGEN Inc., USA) was subcloned into a pQE-2 expression vector at the cut sites of *Nde* I and *Pst* I restriction enzymes. Ligation was performed using T4 Ligase (Thermo Fisher Scientific, USA) at 4°C overnight. The plasmids were inserted into competent *E. coli* TG1 cells using the method described by Chung et al. [19]. The sequence of the cloned *Tpv* HSP 14.3 gene in the recombinant pQE-2 vector (pQE-2/TpvHSP14.3) was confirmed by sequencing (GenScript Biotech., USA). This second variant (*Tpv* HSP 14.3 variant 2) contained the 11-aa extension with 7xHis-tag at the N-termini of *Tpv* HSP 14.3.

Expression and purification of N-terminally modified *Tpv* HSP 14.3 variants. Overnight cultures of the recombinant *E. coli* TG1 cells carrying pQE-31/*Tpv* HSP14.3 and pQE-2/*Tpv* HSP14.3 plasmids were grown in Luria-Bertani (LB) medium supplemented with 100 μg/mL ampicillin at 37°C. When the OD_{600} was reached 0.6, 1 mM of isopropy-β-D-thiogalactoside (IPTG) was added to the culture medium for induction. After cultivation at 37°C for 5 h, cells were collected by centrifugation for 20 min at 4000× *g* and suspended in 50 mM sodium phosphate buffer, pH 8.0 containing 10 mM imidazole and 300 mM NaCI, and then lysed by sonication (Sonics and Materials, USA) at 20 W for 200 s with 30 s intervals. The lysate was centrifuged at 10000× *g* for 30 min at 4°C to obtain soluble fraction. His-tagged fusion proteins with N-terminal extensions of 11-aa or 26-aa, each containing multiple His residues, were purified under native conditions using Ni-NTA affinity chromatography (QIAexpressionist Kit, Qiagen, USA), as previously described [18].

The third N-terminal variant of *Tpv* HSP 14.3 was obtained after N-terminal tag removal by sequential enzymatic digestions at protein level (Fig. 1a). The 11 aa tag of the *Tpv* HSP 14.3 variant 2 was removed by TAGZyme Kit according to the protocol described in the Kit Manual (TAGZYme Kit User Manual, Qiagen, USA), to obtain the variant without tag at the N-terminus (*Tpv* HSP 14.3 variant 3). In this protocol, extra amino acids from the N-terminus of the protein were excised by using dipeptidyl aminopeptidase I (DAPase) in the presence of an excessive amount of glutamine cyclotransferase (Qcyclase) and pyro-glutamyl aminopeptidase (pGAPase). DAPase, Qcyclase, and pGAPase, each having a C-terminal His tag, were then eliminated by small-scale subtractive Ni-NTA chromatography.

Chaperone activity assays. Chaperone-like activities of the *Tpv* HSP 14.3 variants were studied by measuring their capacity to prevent thermal-induced inactivation of the substrate protein at 47°C, as described before [18]. For the heat protection assays, the concentration of the model substrate, pig heart citrate synthase (phCS) (EC 4.1.3.7, Sigma-Aldrich, USA), was adjusted to 0.9 μg/mL using 20 mM Tris-HCl buffer with 1 mM EDTA, pH 8.0 (assay buffer). Diluted phCS samples were then incubated at 47°C for 10 min in the presence of the *Tpv* HSP14.3 variant proteins. After immediate cooling of the mixtures on ice, the remaining phCS activities were measured according to the method of Srere et al. [20]. In these experiments, the reaction mixture (1 mL) in the assay buffer contained 0.2 mM oxaloacetate, 0.15 mM acetyl-CoA and 0.2 mM 5.5'-dithiobis (2-nitrobenzoic acid), 3 μg/mL phCS and 0.45 μg/mL sHSP variant. The increase in the OD_{412} was monitored continuously for 5–10 min using a UV-visible spectrophotometer (Shimadzu, Japan) equipped with a controlled Peltier heater system (Shimadzu, Japan) at 35°C. Initial velocities were computed from activity curves. Control reactions without *Tpv* HSP were also performed with the addition of assay buffer to adjust the total reaction volume. All experiments were conducted in triplicate.

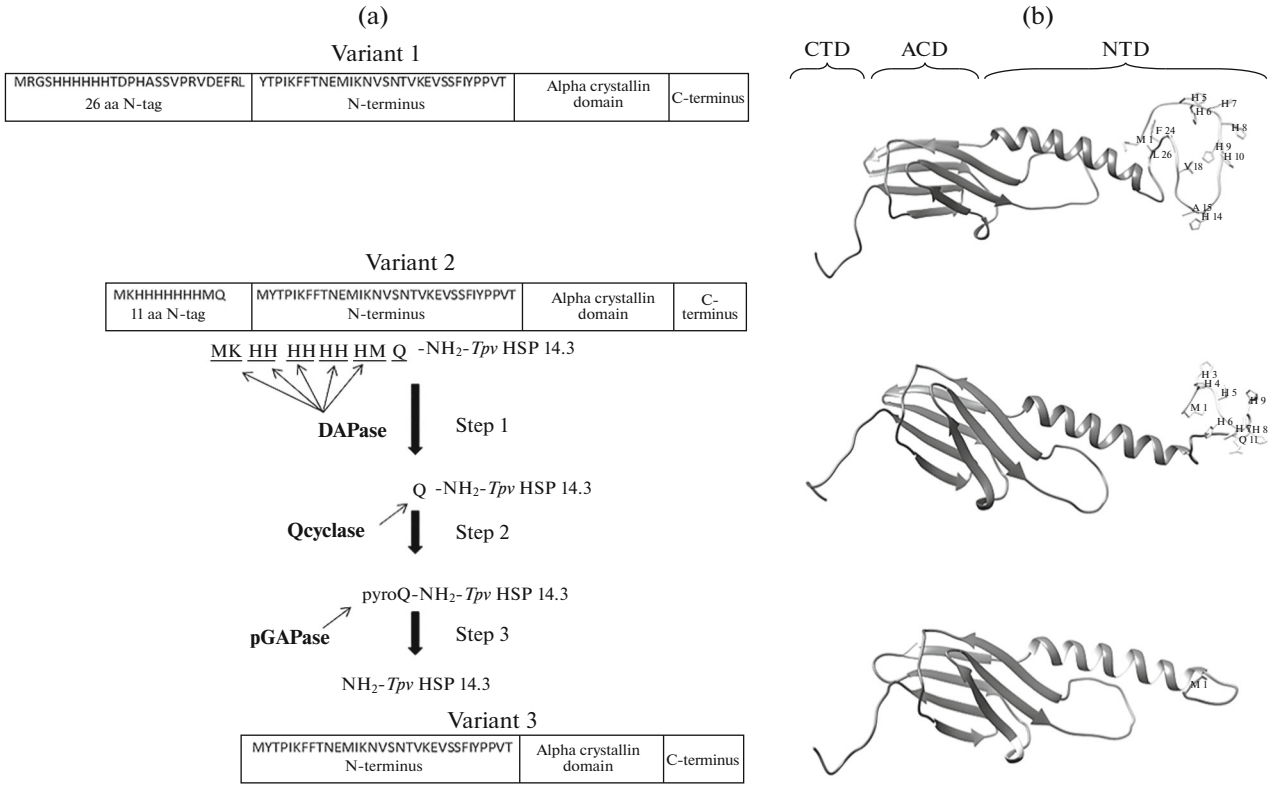

Fig. 1. Schematic presentation of the *Tpv* HSP 14.3 N-terminal constructs and predicted 3D monomeric models. a) N-terminal tag (MKHHHHHHHMQ) of variant 2 was removed by taking advantage of the TAGZyme system in three steps. DAPase I enzyme cleaves dipeptide sequence in pairs in the presence of high amount of Qcyclase until the stop point, Gln (Q). The second enzyme, Qcyclase, converts Gln into pyroglutamine, which was removed by the third enzyme, pGAPase. Thus, the native form of the *Tpv* HSP14.3 protein (variant 3) was obtained. b) 3-D model structures of the three N-terminal variants of the *Tpv* sHSP. NTD: N-terminal domain, ACD: α-crystallin domain, CTD: C-terminal domain.

The effect of pre-heating on the chaperone function of the *Tpv* HSP 14.3 variants was determined by performing the phCS activity assay after heating the samples of *Tpv* HSP variant proteins at 60°C for 10 min, as described above. For data analysis and graphing, GraphPad Prism 9.0 software (GraphPad, USA) was used.

Bioinformatics analysis and three-dimensional structure modelling. The molecular weights of the *Tpv* HSP14.3 variants were predicted with the aid of the ExPASy tool (http://web.expasy.org/compute_pi/). The three-dimensional structure of the *Tpv* HSP 14.3 was generated using homology modeling (MODELLER 9.15 ver) based on crystal structures of *S. tokodaii* (PDB entry 3AAC and 3VQM), *Xanthomonas axonopodis* (PDB entry 3GLA), *Deinococcus radiodurans* (PDB entry 4FEI). Visualization and structure analyses of the models were performed with the UCSF Chimera package (https://www.cgl.ucsf.edu/chimera/).

The intrinsically disordered regions (IDRs) of the N-terminally tagged *Tpv* HSP 14.3 variants and the *Tpv* HSP 14.3 having original NTD were predicted by using the online tool PONDR, which is available at http://www.pondr.com. The threshold value was set to 0.5, and above this value was associated with disorderliness [21]. Hydrophobicity analysis was performed using the Peptide 2.0 tool (https://www.peptide2.com).

RESULTS

Predicted 3-D structure of *Tpv* HSP 14.3 variants and intrinsically disorder region analysis. We generated 3-D structure models of the original form and N-terminally modified forms of *Tpv* HSP 14.3 monomers by homology modeling. The N-termini of all *Tpv* HSP14.3 variants showed a propensity to form α-helical structure while the added N-terminal extensions remained unstructured (Fig. 1b). It is widely accepted that IDRs of the proteins that typically do not fold into a defined tertiary structure consist of a higher proportion of charged or polar amino acids [22]. This notion is supported by our results, which showed that the additional sequences provided by the tags, particularly in variant 1 are enriched in disorder-promoting residues such as R, P, E, S, and L. The content of polar amino acids in the N-terminus of the *Tpv* HSP increased from 15% in the original form (variant 3) to

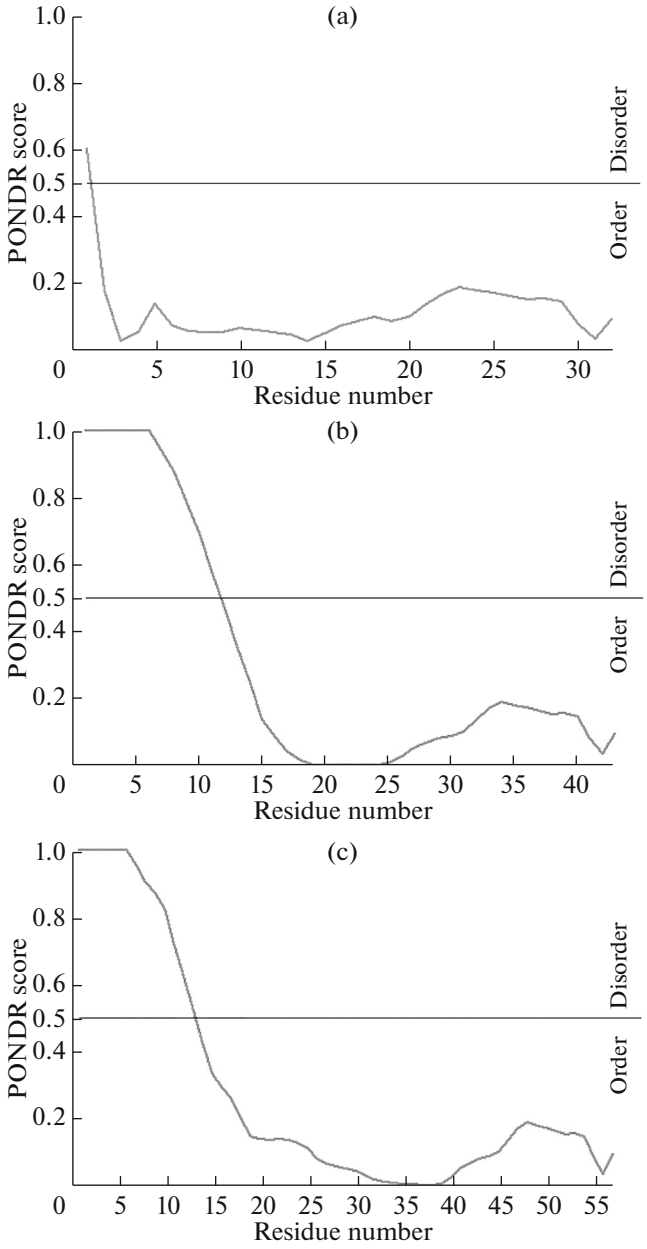

Fig. 2. PONDR score plots of the N-terminal segments of the *Tpv* HSP 14.3 variants. a) *Tpv* HSP 14.3 variant 3 (no extension), b) variant 2 (with 11-aa extension) and c) variant 1 (with 26-aa extension). The straight line shows the threshold that is set at PONDR Score 0.5.

>30% in variant 1 (31.58%) and variant 2 (30.23%). Therefore, the apparent increase in the size of the IDR by the addition of the tags can be attributed to disturbance of the equilibrium between net charge and mean hydrophobicity of the NTD sequence. The graphical representations of the IDRs of the N-termini of the variants obtained using the PONDR predictor are shown in Fig. 2. According to this analysis, only the disorder probability score of the first residue (M) of variant 3 passed the threshold value 0.5. About 3% of

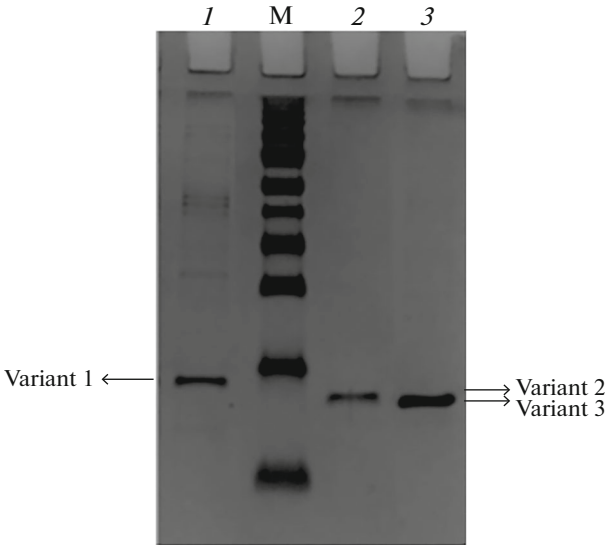

Fig. 3. SDS PAGE analysis for *Tpv* HSP14.3 N-terminal variant proteins. Lane *1*: *Tpv* HSP14.3 with 26-aa tag (variant 1, 17.25 kDa), lane *2*: *Tpv* HSP14.3 with 11-aa tag variant 2, 15.81 kDa), lane *3*: *Tpv* HSP14.3 with no extension (variant 3, 14.32 kDa). Lane M: pre-stained protein ladder.

the N-terminal sequence of this variant exhibited disorderliness. All the added N-terminal tag sequences (11-aa) of variant 2 lie in the disordered region (comprising 25.58% of its NTD). The disordered segment of variant 1 (with 26-aa tag) includes 13-aa of the extended N-terminal sequences (comprising 22.81% of NTD).

SDS-PAGE analysis. The SDS-PAGE results clearly showed that N-terminal fusions of the *Tpv* HSP 14.3 (i.e., variant 1 and variant 2) including poly-His were successfully purified using Ni-NTA affinity chromatography under denaturing conditions (Fig. 3). Removal of the extra 11-aa tag from the variant 2 (MW 15.81 kDa) by exoproteolytic cleavage using TAG-Zyme kit was proved by the presence of the band specific for variant 3 (MW 14.32 kDa) on the gel (Figs. 1a and 3).

Chaperone activity assay with phCS. In order to evaluate the chaperone activity of *Tpv* HSP 14.3 variants with different N-terminal extensions, their ability to protect the model substrate phCS from thermal inactivation at 47°C was examined. The optimal temperature for the mesophilic enzyme phCS is 35°C, and its activity is drastically lost at temperatures above 47°C as previously reported [18]. In agreement with this data, the obtained result demonstrated that in the absence of the chaperone (negative control), phCS enzyme activity decreased about 43-fold (Fig. 4). On the other hand, in the presence of *Tpv* HSP 14.3 variant 1 and variant 2, the remaining phCS activity was about 9.7-fold and 10-fold higher, respectively, than the activity measured in the absence of chaperone. However, removal of the 11-aa N-terminal tag (*Tpv*

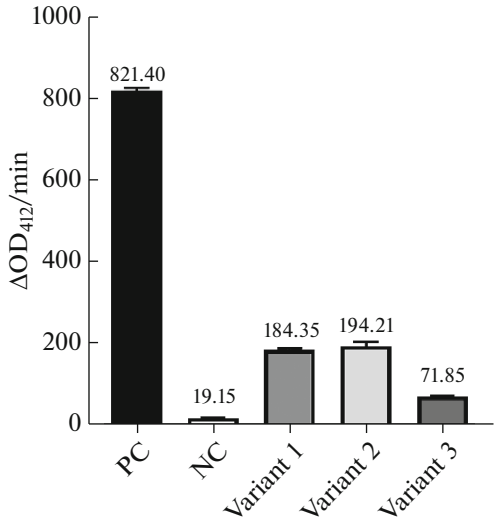

Fig. 4. Chaperone activity assay of *Tpv* HSP 14.3 variants with phCS at 47°C. The remaining activity was monitored by continuously measuring the absorbance at 412 nm. Enzyme activity was expressed as "ΔOD_{412}/min". PC: positive control, activity measured before heat-treatment. NC: negative control, remaining activity after heat treatment in the absence of chaperone. Data represents the average values with ±STD (at the top of each bar) from at least three independent experiments.

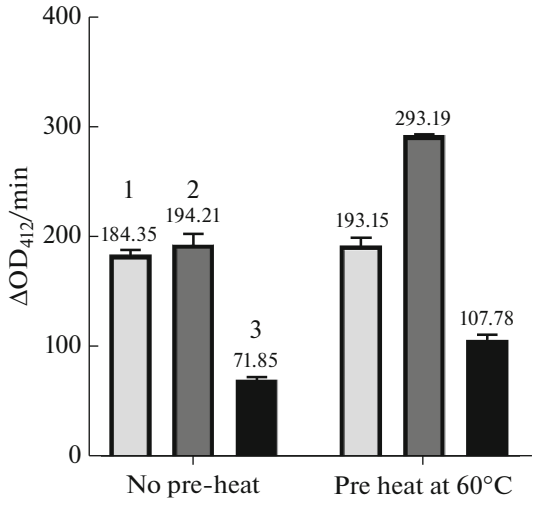

Fig. 5. Effect of pre-heating on chaperone activity of *Tpv* HSP 14.3 variants with phCS. After pre-heating the *Tpv* HSP14.3 variants at 60°C, suppression of the thermal inactivation of the phCS was determined as described in the Materials and Methods. Enzyme activity was expressed as "ΔOD_{412}/min". Light gray columns—variant 1; dark gray columns—variant 2; black columns—variant 3. Data represents the average values with ±STD (at the top of each bar) from at least three independent experiments.

HSP 14.3 variant 3), resulted in an about 3.8-fold increase in the heat protection efficiency of the *Tpv* HSP 14.3, with respect to the negative control. Thus, only 8.7% of the original activity (i.e., of the positive control) could be retained.

Chaperone activity after pre-heat treatment. In order to determine the effect of pre-heating of sHSP on its chaperone activity, the *Tpv* HSP14.3 variants were heated at 60°C for 10 min, then cooled down, before chaperone activity assay was performed. Activity assay using phCS as the substrate was run as described in the Materials and Methods. For all three variants, pre-heating at 60°C resulted in better protection of the phCS activity from heat denaturation at 47°C as compared to non-heated sHSP samples (Fig. 5). Increases in the heat protection efficiencies of all variants after heat induction were from 1.05- to 1.5-fold higher than in the uninduced state.

DISCUSSION

There are several reports suggesting the use of His-tag fusion as an effective means for the purification of various recombinant proteins. In this study, N-terminal fusions of two tags at different sizes and including poly-His have been efficiently used for affinity purification of the *Tpv* HSP 14.3 variants under denaturing conditions (Fig. 3). Some reports indicated that His-tagging may facilitate protein refolding and offer other advantages such as increased protein yield, stability, and solubility [23, 24]. However, there are cases showing that His-tags can affect the structure and/or activity of some proteins adversely and, therefore, are not preferred for crystallographic, physiological studies, or pharmaceutical uses [25]. Until now, the influence of extra N-terminal sequences, such as His-tags, on the chaperone function of sHSPs has not been investigated. In the present study, for the first time, the impact of the poly-His tags of different sizes at the N-terminus on the chaperone activity of the recombinant *Tpv* HSP14.3 HSP was examined. Our results clearly illustrated that protection efficiencies of the *Tpv* HSP 14.3 variant 1 (with 26-aa N-terminus extension) and variant 2 (with 11-aa N-terminus extension) against heat-induced inactivation of the phCS were higher than that of the variant 3 (without NTD extension). Our data from the output of the PONDR predictor suggested that the fused extra residues to the proximal NTD of *Tpv* HSP 14.3 increased its potential to form IDRs due to the additional disorder-promoting amino acids they provided. There are several reports indicating that the structural flexibility of IDRs allows them to interact with a variety of protein partners by adopting different conformations when binding [26–28]. In addition, it was demonstrated that NTD of the sHSPs is structurally disordered with a tendency to form helices, and thus, its hydrophobic residues are presented on a large surface to interact with substrates [9, 29, 30]. In our variant constructs, NTD tags provided additional hydrophobic residues which constitute 30.8 and 18.0% of the 26-aa and 11-aa extensions, respectively. Therefore, the increased potential of the NTD to form

IDRs when tags are fused may provide a greater degree of flexibility and larger exposed surfaces. The latter is most likely presenting hydrophobic residues for efficient binding to substrate protein.

On the other hand, numerous experimental results have shown that chaperone activity of the sHSPs, mainly thermophilic ones, enhanced after pre-heating at high temperatures [9, 31–33]. It was proposed that efficiency of subunit exchange, which is necessary for molecular chaperone activity of the sHSPs, is highly dependent on temperature. At elevated temperatures, sHSPs dissociate into dimers that are amenable to interact with the denatured substrates through their easily accessible hydrophobic surfaces [7, 10, 16, 34, 35]. Consistent with this hypothesis, our experiments also demonstrated that heat induction is an effective strategy for functional activation of the *Tpv* HSP 14.3 variants. Thus, thermal induction together with the increased conformational flexibility of the NTDs should have a significant role in the enhancement of the chaperone activity of sHSPs.

Collectively, the current results indicated a direct correlation between the improved capacity of the NTD to form IDRs and the enhanced heat protection ability of the *Tpv* HSP 14.3. The disorderliness of the NTD may contribute to the high chaperone efficiency of the sHSP, possibly by presenting hydrophobic residues that interact with the hydrophobic patches on the denaturing substrate protein. Therefore, His affinity tags can be an appropriate choice not only for efficient purification of the recombinant sHSPs but also for improvement of their ability to capture substrate proteins and effectively protect them from heat denaturation.

FUNDING

This work was supported with grants from Turkish Scientific and Technical Research Council (TÜBİTAK) (Grant number: 214Z028).

ETHICS APPROVAL AND CONSENT TO PARTICIPATE

This work does not contain any studies involving human and animal subjects.

CONFLICT OF INTEREST

The authors of this work declare that they have no conflicts of interest.

REFERENCES

1. Haslbeck, M. and Vierling, E., *J. Mol. Biol.*, 2015, vol. 427, pp. 1537–1548. https://doi.org/10.1016/j.jmb.2015.02.002
2. Haslbeck, M., Weinkauf, S., and Buchner, J., *J. Biol. Chem.,* 2019, vol. 294, pp. 2121–2132. https://doi.org/10.1074/jbc.REV118.002809
3. Haslbeck, M., Braun, N., Stromer, T., Richter, B., Model, N., Weinkauf, S., et al., *EMBO J.,* 2004, vol. 23, pp. 638–649. https://doi.org/10.1038/sj.emboj.7600080
4. Haslbeck, M., Ignatiou, A., Saibil, H., Helmich, S., Frenzl, E., Stromer, T., et al., *J. Mol. Biol.*, 2004, vol. 343, pp. 445–455. https://doi.org/10.1016/j.jmb.2004.08.048
5. Usui, K., Yoshida, T., Maruyama, T., and Yohda, M., *J. Biosci. Bioeng.,* 2001, vol. 92, pp. 161–166. https://doi.org/10.1016/S1389-1723(01)80218-8
6. Boelens, W.C., *Cell Stress Chaperones,* 2020, vol. 25, pp. 581–591. https://doi.org/10.1007/s12192-020-01093-1
7. Takeda, K., Hayashi, T., Abe, T., Hirano, Y., Hanazono, Y., Yohda, M., et al., *J. Struct. Biol.,* 2011, vol. 174, pp. 92–99. https://doi.org/10.1016/j.jsb.2010.12.006
8. Stamler, R., Kappe, G., Boelens, W., and Slingsby, C., *J. Mol. Biol.,* 2005, vol. 353, pp. 68–79. https://doi.org/10.1016/j.jmb.2005.08.025
9. van Montfort, R.L., Basha, E., Friedrich, K.L., Slingsby, C., and Vierling, E., *Nat. Struct. Biol.,* 2001, vol. 8, pp. 1025–1030. https://doi.org/10.1038/nsb722
10. Stromer, T., Fischer, E., Richter, K., Haslbeck, M., and Buchner, J., *J. Biol. Chem.,* 2004, vol. 279, pp. 11222–11228. https://doi.org/10.1074/jbc.M310149200
11. Fu, X., Zhang, H., Zhang, X., Cao, Y., Jiao, W., Liu, C., et al., *J. Biol. Chem.,* 2005, vol. 280, pp. 6337–6348. https://doi.org/10.1074/jbc.M406319200
12. Jaya, N., Garcia, V., and Vierling, E., *Proc. Natl. Acad. Sci. U. S. A.,* 2009, vol. 106, pp. 15604–15609. https://doi.org/10.1073/pnas.0902177106
13. Basha, E., Friedrich, K.L., and Vierling, E., *J. Biol. Chem.,* 2006, vol. 281, pp. 39943–39952. https://doi.org/10.1074/jbc.M607677200
14. Shashidharamurthy, R., Koteiche, H., Dong, J., and Mchaourab, H.S., *J. Biol. Chem.*, 2005, vol. 280, pp. 5281–5289. https://doi.org/10.1074/jbc.M407236200
15. Rogalla, T., Ehrnsperger, M., Preville, X., Kotlyarov, A., Lutsch, G., Ducasse, C., et al., *J. Biol. Chem.,* 1999, vol. 274, pp. 18947–18956. https://doi.org/10.1074/jbc.274.27.18947
16. Mogk, A., Ruger-herreros, C., and Bukau, B., *Annu. Rev. Microbiol.,* 2019, vol. 73, pp. 89–110. https://doi.org/10.1146/annurev-micro-020518-115515
17. McHaourab, H.S., Lin, Y.L., and Spiller, B.W., *Biochemistry.,* 2012, vol. 51, pp. 5105–5112. https://doi.org/10.1021/bi300525x
18. Kocabıyık, S. and Aygar, S., *Process Biochem.*, 2012, vol. 47, pp. 1676–1683. https://doi.org/10.1016/j.procbio.2011.11.014
19. Chung, C.T., Niemela, S.L., and Miller, R.H., *Proc. Natl. Acad. Sci. U. S. A.,* 1989, vol. 86, pp. 2172–2175. https://doi.org/10.1073/pnas.86.7.2172

20. Srere, P.A., Brazil, H., and Gonen, L., *Acta Chem. Scand.,* vol. 17, pp. 129–134. https://doi.org/10.3891/acta.chem.scand.17s-0129
21. Romero, P., Obradovic, Z., Li, X., Garner, E.C., Brown, C.J., and Dunker, A.K., *Proteins Struct. Funct. Genet.,* 2001, vol. 42, pp. 38–48. https://doi.org/10.1002/1097-0134(20010101)42:1<38::AID-PROT50>3.0.CO;2-3
22. Morris, O.M., Torpey, J.H., and Isaacson, R.L., *Open Biol.,* 2021, vol. 11. https://doi.org/10.1098/rsob.210222
23. Amor-Mahjoub, M., Suppini, J.P., Gomez-Vriely-unck, N., and Ladjimi, M., *J. Chromatogr. B. Anal. Technol. Biomed. Life Sci.,* 2006, vol. 844, pp. 328–334. https://doi.org/10.1016/j.jchromb.2006.07.031
24. Sun, Q.M., Chen, L.L., Cao, L., Fang, L., Chen, C., and Hua, Z.C., *Biotechnol. Prog.,* 2005, vol. 21, pp. 1048–1052. https://doi.org/10.1021/bp049583x
25. Schäfer, F., Schäfer, A., and Steinert, K., *J. Biomol. Tech.,* 2002, vol.13, pp. 158–171.
26. Oldfield, C.J., Meng, J., Yang, J.Y., Qu, M.Q., Uversky, V.N., and Dunker, A.K., *BMC Genomics,* 2008, vol. 9, pp. 1–20. https://doi.org/10.1186/1471-2164-9-S1-S1
27. Russell, R.B. and Gibson, T.J., *FEBS Lett.,* 2008, vol. 582, pp. 1271–1275. https://doi.org/10.1016/j.febslet.2008.02.027
28. Wright, PE. and Dyson, HJ., *Curr. Opin. Struct. Biol.,* 2009, vol. 19, pp. 31–38. https://doi.org/10.1016/j.sbi.2008.12.003
29. Kim, K.K., Kim, R., and Kim, S.H., *Nature,* 1998, vol. 394, pp. 595–599. https://doi.org/10.1038/29106
30. Webster, J.M., Darling, A.L., Uversky, V.N., and Blair, L.J., *Front. Pharmacol.,* 2019, vol. 10, pp. 1–18. https://doi.org/10.3389/fphar.2019.01047
31. Usui, K., Ishii, N., Kawarabayasi, Y., and Yohda, M., *Protein Sci.,* 2004, vol.13, pp. 134–144. https://doi.org/10.1110/ps.03264204
32. Bova, M.P., Huang, Q., Ding, L., and Horwitz, J., *J. Biol. Chem.,* 2002, vol. 277, pp. 38468–38475. https://doi.org/10.1074/jbc.M205594200
33. Haslbeck, M., Walke, S., Stromer, T., Ehrnsperger, M., White, H.E., Chen, S., et al., *EMBO J.,* 1999, vol. 18, pp. 6744–6751. https://doi.org/10.1093/emboj/18.23.6744
34. Kim, R., Lai, L., Lee, H.H., Cheong, G.W., Kim, K.K., Wu, Z., et al., *Proc. Natl. Acad. Sci. U. S. A.,* 2003, vol. 100, pp. 151–155. https://doi.org/10.1073/pnas.1032940100
35. Abe, T., Oka, T., Nakagome, A., Tsukada, Y., Yasunaga, T., and Yohda, M., *J. Biochem.,* 2011, vol. 150, pp. 403–409. https://doi.org/10.1093/jb/mvr074